

Theoretical Examination of the Lithium Depletion Boundary

Christopher J. Burke and Marc H. Pinsonneault

*Astronomy Department, The Ohio State University, 140 W. 18th Ave., Columbus, OH
43210;*

cjburke@astronomy.ohio-state.edu, pinsono@astronomy.ohio-state.edu

and

Alison Sills

*Department of Physics and Astronomy, McMaster University, 1280 Main Street West,
Hamilton, Ontario, Canada, L8S 4M1;*

asills@physics.mcmaster.ca

ABSTRACT

We explore the sensitivity in open cluster ages obtained by the lithium depletion boundary (LDB) technique to the stellar model input physics. The LDB age technique is limited to open clusters with ages ranging from 20 to 200 Myr. Effective $1\text{-}\sigma$ errors in the LDB technique due to uncertain input physics are roughly 3% at the oldest age increasing to 8% at the youngest age. Bolometric correction uncertainties add an additional 10 to 6% error to the LDB age technique for old and young clusters, respectively. Rotation rates matching the observed fastest rotators in the Pleiades affect LDB ages by less than 2%. The range of rotation rates in an open cluster are expected to “smear” the LDB location by only 0.02 mag for a Pleiades age cluster increasing to 0.06 mag for a 20 Myr cluster. Thus, the observational error of locating the LDB ($\sim 7\text{-}10\%$) and the bolometric correction uncertainty currently dominate the error in LDB ages. For our base case, we formally derive a LDB age of 148 ± 19 Myr for the Pleiades, where the error includes 8, 3, and 9% contributions from observational, theoretical, and bolometric correction sources, respectively. A maximally plausible 0.3 magnitude shift in the I-band bolometric correction to reconcile main sequence isochrone fits with the observed (V-I) color for the low mass Pleiades members results in an age of 126 ± 11 Myr, where the error includes observational and theoretical errors only. Upper main-sequence-fitting ages that do not include convective core overshoot for the Pleiades (~ 75 Myr) are ruled out by the LDB age technique.

Subject headings: stars: low-mass, brown dwarfs—stars: pre-main sequence—stars: rotation—open clusters and associations: general

1. Introduction

Accurate ages for nearby stellar clusters are the basic observational templates that constrain the formation history of our Galaxy and the Universe. Unfortunately, theoretical isochrones fit to the upper main sequence provide absolute ages for the most thoroughly studied young open clusters that are still uncertain by a factor of two (Stauffer et al. 2000). The uncertainty mainly results from the dependence of the lifetime of massive stars on the size of their convective cores. Convective core overshoot brings fresh hydrogen-rich material to the core, extending the stellar lifetime on the main sequence. As a result, cluster age estimates are quite sensitive to the degree of convective core overshoot in the theoretical calculations. There is evidence that the inclusion of convective core overshoot results in an improved agreement between theoretical evolution rates and number counts in the Hertzsprung gap, and also an improved fit to the width of the main sequence turnoff in open clusters (Andersen, Nordström, & Clausen 1990; Demarque, Sarajedini, & Guo 1994). Thus, theoretical calculations that include convective core overshoot result in an older absolute age scale relative to theoretical calculations that do not. Calibrating the older convective core overshoot age scale requires an independent technique for determining stellar cluster ages. Lithium depletion age dating is one possibility, and in this paper we discuss the reliability of this technique.

The lithium depletion boundary (LDB) technique is an independent method to determine the age of open clusters with ages that range from 20 to 200 Myr. Proton reactions destroy Li^7 near a destruction temperature, $T_D \sim 2.5 \times 10^6$ K, easily obtained under stellar conditions. In general, the presence or absence of photospheric lithium determines whether sufficient time has passed for a majority of the stellar material to reach depths in the star where $T=T_D$. For stars that are fully convective during pre-main-sequence contraction ($M \lesssim 0.4 M_\odot$), the convective overturn timescale is much less than the evolutionary timescale, and the entire lithium content is rapidly destroyed when the stellar core temperature, T_C , reaches T_D . Since the rate at which the core temperature increases to the destruction temperature is a strong function of stellar mass, spectral observations of Li^7 in fully convective stars during pre-main-sequence contraction is an accurate age diagnostic. Higher mass stars reach the condition $T_C = T_D$ at an earlier age and higher luminosity than lower mass stars, and the lithium abundance decreases by a factor of 100 over a very narrow luminosity.

LDB ages have been obtained for several young open clusters: the Pleiades, Alpha Per, IC 2391, & NGC 2547 (Stauffer, Schultz, & Kirkpatrick 1998; Stauffer et al. 1999; Barrado y Navascués, Stauffer, & Patten 1999; Oliveira et al. 2003). In an independent analysis, Jeffries & Naylor (2000) verified the conclusions of the previous open cluster studies that the LDB ages are ~ 1.6 times older than upper main-sequence-fitting ages without convective

core overshoot. Jeffries & Naylor (2000) find that the observational uncertainties (locating the LDB, photometric calibrations, distance, and reddening) are larger than the theoretical uncertainties (choice of model and bolometric corrections) for the Pleiades ($\sigma_{obs} \sim 16\%$; $\sigma_{thy} \sim 9\%$, respectively). However, Jeffries & Naylor (2000) point out that the theoretical errors may not be complete, since common assumptions made by several independent theoretical calculations used in this study may hide additional systematics. They also point out that non-negligible errors may be associated with the bolometric corrections.

Bildsten et al. (1997) provide the most detailed quantitative estimate of the uncertainties in LDB calculations. The Bildsten et al. (1997), analytical lithium depletion model consists of a fully convective polytrope contracting at constant effective temperature. A comparison of their analytical model to detailed numerical calculations results in maximum differences in the LDB ages of 25% from Chabrier, Baraffe, & Plez (1996) and 15% from D’Antona & Mazzitelli (1994), demonstrating the robustness of the LDB technique to uncertain input physics. D’Antona & Mazzitelli (1997) comment on the LDB ages being “practically independent on the details of the models including the opacity”. However, they do not go into quantitative detail.

In this paper we determine the size of errors in the LDB technique that result from theoretical errors in the lithium depletion calculations and uncertainties in the bolometric corrections. We can then determine the dominant error source in the LDB age technique and confirm whether the discrepancy between the upper main-sequence-fitting ages and LDB ages is real. Employing the Yale Rotating Stellar Evolution Code (YREC), we compare the lithium depletion calculations using up-to-date input physics to models using older generation equations of state, opacities, and atmospheres as well as variations in the mixing length and metallicity. The difference in LDB ages that results from employing older generation input physics allows us to ascertain the expected deviations of the LDB ages from up-to-date input physics. Additionally, we quantify the impact of stellar rotation and various bolometric correction determinations on LDB ages.

In Section 2 we briefly describe the YREC stellar model and determine our reference LDB-luminosity-age relation obtained with the latest input physics. Section 3 examines the robustness of the LDB to variations in the input physics. Then, we discuss the error budget in the LDB ages due to input physics uncertainties in Section 4. In Section 5 we compare the reference LDB calculations to other calculations in the literature. The error budget in the LDB ages derived from the comparisons with other calculations in the literature and the final adopted theoretical error in the LDB ages is discussed in Section 6. Section 7 is devoted to the significant uncertainties in the I-band bolometric correction. In Section 8 we summarize our results and derive new LDB ages with improved errors for the open clusters

with previous LDB age determinations.

2. Reference Model

In this section we describe the lithium depletion calculations and the input physics that define our reference LDB-luminosity-age relation. This reference relation serves as the standard to quantify the uncertainty in LDB ages. We use the Yale Rotation Evolution Code (YREC) (Sills, Pinsonneault, & Terndrup 2000) for all stellar model calculations. For the reference calculation, we select standard, non-rotating, solar-calibrated stellar models with masses that range from 0.065 to 0.30 M_{\odot} . The upper mass limit ensures full convection during lithium depletion and minimizes the impact of initial conditions. Through accretion and mass loss, a star interacts with its surroundings during the earliest phases of its life. However, any structural changes to the star that may occur due to this complex interaction with its surroundings is erased after several Kelvin-Helmholtz time scales. The Kelvin-Helmholtz time scale for our $M=0.3 M_{\odot}$ starting model is one-tenth of the time for lithium depletion, making these complications negligible. Stars with $M \leq 0.06 M_{\odot}$ never reach temperatures high enough to destroy lithium completely (D’Antona & Mazzitelli 1994), and our reference calculations confirm this fact. The above mass limits constrain the validity of the LDB age technique to stellar populations with ages between 20 and 200 Myr. For clusters with ages less than 20 Myr, the uncertain initial conditions, deuterium burning, and adopted zero-age (which all occur on timescales of a few 10^6 years) become an increasing fraction of the LDB age. For clusters with ages older than 200 Myr, lithium is depleted over a larger width of luminosity, and lacks a clearly defined LDB.

Adopting a solar metallicity, $Z=0.0188$, and the heavy element mix of Grevesse & Noels (1993), we determine the ratio of mixing length parameter to pressure scale height and helium abundance by calibrating to the solar data, resulting in $\alpha \equiv l_m/H_p = 1.75$ and $Y=0.27$, respectively. We use the OPAL equation of state from Rogers, Swenson, & Iglesias (1996) where it is available and the equation of state of Saumon, Chabrier, & Van Horn (1995) otherwise. We investigate the effect of the latest OPAL 2001 equation of state (Rogers & Nayfonov 2002) on the LDB ages in Section 3.2. The low temperature atmospheres of Hauschildt, Allard, & Baron (1999) provide the pressure at $T=T_{\text{eff}}$, which we apply as the outer boundary condition.

Physical conditions in low mass stars fall outside opacity tables employed to model solar-type stars. Figure 1 shows several stellar density profiles as a function of temperature for the low mass stellar regime applicable to this study. The two solid lines trace the run of density for the 0.3 M_{\odot} reference models at the initial and lithium depletion epochs;

lower and higher density, respectively. The two dashed lines show the density evolution for the $0.065 M_{\odot}$ reference model. The dotted lines represent the various opacity table boundaries. The diagonal dotted line in Figure 1 shows the upper density boundary at $R \equiv \rho/T_6^3 = 1$ for the Alexander & Ferguson (1994) low temperature and Iglesias & Rogers (1996) high temperature opacities used in the reference calculations. A linear ramp between $4.0 \lesssim \log(T) \lesssim 4.1$ provides a smooth transition between the two opacity tables. For the reference model, we supplement the Alexander & Ferguson (1994) low temperature opacity toward higher densities with the molecular opacity table of Alexander, Johnson, & Rypma (1983). In Figure 1, the dotted line starting at $\log(T)=4.0$ with an uneven upper-density boundary toward lower temperatures outlines the Alexander, Johnson, & Rypma (1983) molecular opacity table. A linear ramp toward higher densities over 1 dex starting at the $R=1$ boundary is used to transition smoothly between the Alexander & Ferguson (1994) and Alexander, Johnson, & Rypma (1983) opacities. A linear extrapolation in density provides the opacity for densities higher than the table boundaries.

The OPAL opacity table (Iglesias & Rogers 1996) and OPAL equation of state (Rogers, Swenson, & Iglesias 1996) share the same $R=1$ boundary shown in Figure 1. For densities higher than the $R=1$ boundary, we apply a linear ramp constant in density to transition to the Saumon, Chabrier, & Van Horn (1995) equation of state. The ramp has a width of the final two density values of the OPAL table. The OPAL equation of state also has a low-temperature boundary at $\log(T)=3.75$ K. For temperatures below the $R=1$ boundary, we transition to the Saumon, Chabrier, & Van Horn (1995) equation of state with a linear ramp starting at $\log(T)=3.80$ K.

We update the conductive opacities with the extensive calculations from Potekhin, Chabrier, & Yakovlev (1997) and Potekhin et al. (1999). Their conductive opacity calculations are for a fully ionized single-ion species. We follow the procedure given in Potekhin et al. (1999) to calculate an arbitrary mixture for the conductive opacity by expressing the electron-ion collision frequency as a summation over the coulomb logarithm factors for the ion species present. We assume singly ionized O^{16} for the entire stellar metal content. H and He are assumed fully ionized, valid since in the unionized regime, $\log(\rho) \lesssim 0.0$ and $\log(T) \lesssim 4.0$, conduction is inefficient and the radiative opacity dominates.

The initial stellar models start at the deuterium-burning birthline (Stahler 1988). We obtain our deuterium birthline by starting a stellar model high up on the Hyashi track and designate the birthline when the core temperature reaches the same core temperature when deuterium decreases by a factor of 100 in the calculations of D’Antona & Mazzitelli (1994) (see their Table 7). Since deuterium burning completes in $\lesssim 3\%$ of the time for lithium depletion, our results are insensitive to the adopted initial conditions.

Using the above mentioned input physics, we calculate a reference relation for the luminosity and age when lithium is depleted by a factor of 100 from its initial value. The lithium depletion ages are systematically 15% and 6% younger at fixed luminosity for adopting a lithium depletion by a factor of 2 and 10, respectively. As we quantify in the following sections, the systematic LDB age difference associated with adopting a different lithium depletion factor is similar in size to errors associated with the input physics uncertainty. Thus, comparisons with other lithium depletion calculations require a common depletion factor.

We find the LDB age is sensitive to numerical time resolution. Insufficient time resolution results in systematically older lithium depletion ages. Halving the time resolution iteratively until the lithium depletion age varies by less than 1% ensures the time-resolution numerical systematic error is negligible. Doubling the spatial resolution of our reference calculation results in no impact on the derived LDB ages as a function of luminosity. When examining the sensitivity of the LDB ages to changes in the input physics, all LDB age variations are given as deviations from this reference model. The reference LDB-luminosity-age relation is shown in Figure 2. The relation in tabular form is given in Table 1.

3. Input Physics Uncertainties

In this section we determine the error in the LDB-luminosity-age relation that results from uncertainties in the model input physics. We quantify the theoretical uncertainty by varying the input physics of our reference model. The following subsections describe each physical input in turn.

3.1. Mixing Length

Our models employ the mixing length theory for convective transport (Vitense 1953). As in our reference models, the mixing length parameter is commonly adjusted to fit the solar data. However, without a physical model for the mixing length parameter, the solar calibrated model may not be applicable to stars of a different mass (Ludwig, Freytag, & Steffen 1999). Other studies (Baraffe et al. 1998) adopt the mixing length to be equal to the pressure scale height, $\alpha = 1.0$, for the interior calculation in order to match the $\alpha = 1.0$ employed in the atmosphere (Hauschildt, Allard, & Baron 1999).

The temperature gradient only becomes sensitive to the adopted mixing length parameter in the superadiabatic zone of the low density envelope. The deep interior of the star has vigorous convection characterized by the temperature gradient, $\nabla = \nabla_{ad}$ (Kippenhahn

& Weigert 1990). The over-adiabacity, $x \equiv \nabla - \nabla_{ad}$, of the stellar envelope depends on the mixing length parameter with a range of powers from $x \propto l_m^{0.0}$ to $x \propto l_m^{-1/3}$. Thus, for two stars with the same central temperature, the star with the smaller mixing length will always have a larger temperature gradient leading to a cooler surface temperature and an older LDB age.

Figure 3 quantifies the effect on the LDB age of reducing the mixing length parameter from the reference model’s value, $\alpha = 1.75$, to $\alpha = 1.0$. The solid line in Figure 3 shows the difference in age between the reduced-mixing-length LDB-luminosity-age relation and the reference LDB-luminosity-age relation as a percentage of the reference model LDB age at fixed luminosity. All comparisons between models are at fixed luminosity, since the luminosity of the LDB is the observed quantity. A positive difference is in the sense that reducing the mixing length parameter leads to older LDB ages at fixed luminosity than the reference model.

The mixing-length formalism is a 1-D static approximation of a phenomena that is intrinsically 3-D and time dependent. Thus, it may not be an accurate representation of convection. Computational limitations prevent a full 3-D parameter-free convection implementation making it difficult to fully quantify the shortcomings of the mixing-length formalism in determining the LDB ages. Some constraints can be placed by comparing our calculations to other calculations in the literature that implement alternative 1-D static convection treatments. The LDB calculations of D’Antona & Mazzitelli (1994) implement the Canuto & Mazzitelli (1991) convective theory and D’Antona & Mazzitelli (1997) implement the convection theory outlined in Ventura et al. (1998). Our calculation of enforcing the adiabatic temperature gradient (Section 3.3), bypassing the convection theory, provides another handle on the impact the convection theory has on LDB ages

For the remaining variations to the input physics, unless otherwise stated, we recalibrate the mixing length and helium to match the solar data. The recalibration does not significantly affect the LDB calculation. For example, in the case of using a gray atmosphere (see Section 3.4), the LDB age difference at the highest luminosity would be 4.5% with a recalibration of the mixing length instead of 5.0% without recalibrating the mixing length.

3.2. Equation of State

The reference models employ the Iglesias & Rogers (1996) equation of state and are supplemented toward lower temperatures and higher densities by the Saumon, Chabrier, & Van Horn (1995) equation of state. One alternative equation of state valid in the low

mass regime is the MHD equation of state by Däppen et al. (1988). Unfortunately, the density upper limit, $\log \rho = -2.0$, of the MHD equation of state prevents calculations to the lithium depletion age for $M/M_{\odot} < 0.175$. For consistency we recalibrate the mixing length parameter, $\alpha = 1.75$, and helium abundance, $Y=0.272$, to match the solar data using the MHD equation of state. The dashed line in Figure 3 shows the MHD equation of state results in older LDB ages, $\sim 2\%$, over the restricted mass range. This line is offset slightly for clarity.

Recently, the OPAL group updated their equation of state. The latest equation of state, OPAL 2001, treats the electrons relativistically, improves the activity expansion method for repulsive inter-particle interactions, and covers a larger range in temperature and density (Rogers & Nayfonov 2002). The dot-dashed line in Figure 3 shows the impact on LDB ages using the OPAL 2001 equation of state. Despite the improved coverage of temperature and density, the table is still inadequate for evolution to the lithium depletion boundary for $M < 0.08M_{\odot}$. As a side note, evolution to the main sequence is only possible for $M > 0.125M_{\odot}$ using the OPAL 2001 equation of state only.

Uncertainties in the low density, high temperature regime covered by the Iglesias & Rogers (1996) calculations have a negligible impact on LDB ages. Using the Saumon, Chabrier, & Van Horn (1995) equation of state in place of Iglesias & Rogers (1996) results in no change to the LDB age. For completeness, we calculate LDB ages using an older generation equation of state based on the Saha equation with Debye-Hückel corrections (Guenther et al. 1992). The Saha equation of state results in 50% older LDB ages over a limited mass range, $M \gtrsim 0.2M_{\odot}$. The calculation becomes numerically unstable for lower masses. Use of the Saha equation of state for a solar model also results in a poor fit to solar oscillation data (Guenther et al. 1992). For the above reasons, the Saha equation of state is too simplistic for realistic calculations and is not included in the overall error budget.

3.3. Opacity

In stellar models, the radiative opacity determines the temperature gradient in regions where energy is transported by radiation and to a lesser degree determines the temperature gradient in superadiabatic convective regions. In the mass range relevant to the LDB, efficient convection transports energy over $\sim 98\%$ of the stellar mass. Thus, radiative opacities become important in determining the stellar structure of the remaining 2% of the stellar mass. Unfortunately, molecular dissociation and ionization greatly complicate the opacity calculations in these outer regions.

As shown in Figure 1, the commonly used low temperature opacities of Alexander & Ferguson (1994) are insufficient to model the superadiabatic and possible radiative zones present in the low mass stars of this study. The diagonal dotted line shows the upper density limit of the Alexander & Ferguson (1994) opacity data. Thus, for the reference models we supplement the Alexander & Ferguson (1994) low temperature opacity data toward higher densities with the molecular opacities of Alexander, Johnson, & Rypma (1983) as described in Section 2. Energy transport of the stellar interior follows the adiabatic temperature gradient, so any changes in the opacities at high temperatures, $\log(T) \gtrsim 4.0$, are inconsequential to the LDB. Thus, only low temperature opacities are varied in this study. When varying the low temperature opacity of the envelope, we are unable to use a self-consistent atmosphere that employs the same alternative opacity.

As a limiting case, we show the effect of enforcing the adiabatic temperature gradient throughout the stellar interior, essentially ignoring the mixing length theory, as the solid line in Figure 4. The superadiabatic region is eliminated, leading to a smaller temperature gradient and hotter star, which evolves more rapidly.

For alternative low temperature opacities, we first considered replacements to the more uncertain high density, $R > 1$, molecular opacities of Alexander, Johnson, & Rypma (1983). However, the stellar envelope evolves roughly perpendicular to the $R=1$ opacity boundary (see Figure 1). Using opacity tables that contain large systematic differences at the $R=1$ transition region can lead to rapid variations in the entropy structure of the outer envelope. The increase or decrease in the size of radiative and superadiabatic zones can enhance or reduce the rate of evolution as described in Guillot et al. (1995). Thus, patching two opacity tables together can artificially affect the rate of evolution. Fortunately, our selection of tables in the reference models results in a smooth transition, and the effect on our reference models is negligible. To quantify the impact, we calculate LDB ages with opacities toward higher densities obtained by a linear-in-log-space extrapolation of the Alexander & Ferguson (1994) opacities. The difference in LDB ages is less than 1% over the entire mass range.

The above discussion emphasizes the importance of continued work in the low temperature opacities for self-consistent calculations over a wider range in density. For the comparisons that follow, we use a single opacity table and perform the linear extrapolation toward higher densities if necessary. The low temperature opacity table is connected to the high temperature opacity at $\log(T)=4.0$, and the high opacity and high density at the boundaries of these opacity tables ensure convective transport of energy. Additionally, hydrogen ionization dominates the opacity at the boundary between the high and low temperature opacities. Thus, tables of differing metal abundances match well.

Kurucz (1998) provides an alternative opacity calculation in the low temperature

regime. We show its impact on the LDB ages as the dashed line in Figure 4. The opacity data have the same $R=1$ boundary as the Alexander & Ferguson (1994) opacities, and are extrapolated toward higher densities. The mixing length and helium are recalibrated to the solar data yielding $\alpha = 1.731$ and $Y = 0.272$, respectively. The Kurucz (1998) and Alexander & Ferguson (1994) opacities are very similar except for $\log(T) < 3.6$, where the effects of molecules become important. The opacities of Alexander & Ferguson (1994) are increasingly larger for $\log(T) < 3.6$ in comparison to the Kurucz (1998) opacity data. The lower Kurucz (1998) opacities in the outermost layers lead to a hotter star, which evolves more rapidly.

We compare our reference models to models using the latest opacity calculations of Allard et al. (2001) as the short-dashed line in Figure 4. Figure 4 shows the comparison between a calculation employing the so-called "dusty" opacities that include the affects of dust grains on the opacities to the reference calculation. The "dusty" opacity table fully covers the low temperature regime under investigation here. The solar calibration yields $\alpha = 1.767$ and $Y = 0.272$. We also calculate LDB ages using the so-called "condensed" opacities of Allard et al. (2001) that remove grains from the opacity since they condense out of the photosphere. Since the models are never cool enough for grain formation, neither the "dusty" opacities or "condensed" opacities appreciably affect the LDB ages.

The opacity tables presented so far have qualitatively similar structure. The opacities have a maximum at $\log(T)=4.4$ due to hydrogen ionization and sharply decrease toward cooler temperatures with a minimum at $\log(T)\sim 3.3$. The opacities begin to increase toward even cooler temperatures due to the formation of molecules and collision-induced absorption. Also, there is an overall increase in the opacities toward higher density. Following advances in more complete line lists, the overall opacity tends to increase. In order to study the impact of higher opacities and the possibility of a change in the qualitative shape to the opacity data, we create an opacity table that is identical to the reference calculation opacities for temperatures greater than $\log(T)=4.0$. For temperatures less than $\log(T)=4.0$, the opacities at fixed density are extrapolated toward lower temperatures at a constant value given by the opacity value at $\log(T)=4.0$ for the corresponding density. Thus, the only structure kept is the increase in opacity for increasing density.

The dot-dashed line in Figure 4 shows the resulting LDB ages using the extreme high opacity table described in the preceding paragraph and a solar-calibrated $\alpha = 2.096$ and $Y = 0.271$. The higher opacities do increase the superadiabatic temperature gradient, which results in cooler stars. However, there is only a modest increase in the LDB ages. The opacities are currently high enough that the stars are strongly convective all the way to the atmosphere boundary point.

In the opposite opacity extreme, we calculate LDB ages for a zero-metallicity opacity (Stahler, Palla, & Salpeter 1986). The solar calibration results in $\alpha = 1.50$ and $Y = 0.271$. The significant reduction in the LDB ages for the zero-metallicity opacity is shown as the dotted line in Figure 4. The effective temperature is 20 to 30% larger than the reference case. These low and high opacities are obviously extreme and unphysical, but they set limiting cases.

One additional note on the topic of opacity, we confirm the findings of Chabrier et al. (2000), that conductive energy transport only affects later stages of evolution than the lithium depletion and has no impact on the LDB ages.

3.4. Atmosphere & Boundary Condition

Even though a standard gray atmosphere results in unrealistically high effective temperatures in the mass regime studied here, it provides an extreme case for deviations from the reference calculation, which employs the Hauschildt, Allard, & Baron (1999) atmosphere. For the gray atmosphere, we use the reference calculation’s mixing length and helium. The impact on the lithium depletion relation is shown as the solid line in Figure 5. The LDB age is 5% younger for the highest luminosity and is negligibly different for the lowest luminosity. There are few alternatives to the gray atmosphere and Hauschildt, Allard, & Baron (1999) atmosphere for modeling low-mass stars. Comparisons to other independent LDB calculations in Section 5 provide some constraints on the impact alternative atmospheres can have on the LDB ages.

The Hauschildt, Allard, & Baron (1999) atmosphere limits calculations to solar metallicity. To check the impact of metallicity variations on the LDB ages, we use the gray atmosphere for a nonsolar-metallicity calculation. A gray-atmosphere calculation using a metallicity that is increased by 0.1 dex (assuming $\Delta Y/\Delta Z=2.0$) results in a less than 2% increase in the LDB ages over all luminosities when compared to the gray-atmosphere calculation at solar metallicity.

The atmosphere provides the outer boundary conditions required for the stellar interior calculation. Our reference calculation fixes the boundary condition at an optical depth where the temperature is equal to the effective temperature. This optical depth is close to $\tau = 2/3$. In their calculation of low mass stellar models, Baraffe et al. (1998) choose a deeper $\tau = 100$ boundary condition. They prefer the deeper boundary condition to ensure the interior calculation is in the fully-adiabatic regime and to reduce the extrapolation of the opacity data.

It is unclear which of these fitting points is more appropriate. In our case of the shallow $\tau = 2/3$ boundary condition, the potential of a mismatch between the interior and atmosphere opacity data resulting in abrupt variations to the convective stability criterion or overradiabicity exists. Whereas the deeper $\tau = 100$ boundary condition reduces this problem, it has a disadvantage since the atmosphere calculations of Hauschildt, Allard, & Baron (1999) do not include real gas effects in the equation of state. The mismatch between the interior Saumon, Chabrier, & Van Horn (1995) equation of state and Hauschildt, Allard, & Baron (1999) equation of state can be as large as 1.6% in density at $\tau = 100$, whereas the mismatch is $<0.9\%$ in density at $\tau = 2/3$. In summary, both of these fitting points are equally valid and neither is ideal. To quantify the impact on the LDB ages due to variations in the boundary condition depth, we calculate the LDB using $\tau = 100$. This results in a 3% younger LDB for the oldest clusters and a 10% older LDB age for the youngest clusters (dashed line - Figure 5).

3.5. Rotation

Rotation affects LDB ages in several ways. The change in kinetic energy of rotation enters the energy generation equation, and rotation provides additional pressure support which can alter the effective temperature and thus the rate of gravitational contraction. Current observations and theory suggest the rotational evolution of a star begins with efficient angular momentum loss via a disc-locking mechanism to nearly constant angular momentum evolution to again efficient angular momentum loss via a stellar wind (Stassun & Terndrup 2003). Due to the complicated rotational evolution of a star we investigate two limiting cases of evolution at constant angular momentum and evolution with significant amounts of angular momentum loss. As a guide for these two cases we match the model rotation rates to the observed upper envelope of rotation rates in the Pleiades open cluster (Terndrup et al. 2000). The upper envelope of rotation rates is approximated by a linear decrease in $V \sin i$ from $V \sin i = 70 \text{ km s}^{-1}$ at $M = 0.3 M_{\odot}$ to $V \sin i = 50 \text{ km s}^{-1}$ at $M = 0.1 M_{\odot}$ (see Figure 7 of Terndrup et al. (2000)). The model rotation rates are extrapolated toward lower masses. We assume $\sin i = \pi/4$ to obtain the physical rotation rate.

For evolution without angular momentum loss, rotation rates are matched to the Pleiades rotation rates at an age of 120 Myr. Since the stars evolve at constant angular momentum and spin up as their radii contract, adopting an older age for the Pleiades (self-consistent with the LDB age derived in Section conclude) would reduce the impact of rotation even further. The no angular momentum loss evolution results in 2% older ages for the minimum LDB mass and $< 1\%$ older ages for higher masses. Previous claims of 20% older LDB ages

result from allowing a rotation rate greater than 200 kms^{-1} at the Pleiades age for the minimum LDB mass (Burke & Pinsonneault 2000). Such high rotation rates are only observed for solar-mass stars, and our adopted 65 kms^{-1} rotation rate at Pleiades age in this study is more appropriate for the lower mass stars relevant to the LDB ages.

Our second limiting case for the rotational evolution examines the impact of efficient angular momentum loss. The stars are forced to evolve at a constant rotational velocity matched to the Pleiades rotation rates as described in the preceding paragraph up to an age of 120 Myr and henceforth evolve at constant angular momentum. This results in 2% younger ages for the minimum LDB mass and 6% younger ages for the highest LDB mass.

Open cluster members of a given mass have a wide range of rotation rates which indicates a variety of evolutionary sequences (Terndrup et al. 2000). Thus an open cluster of a given age may have a less well defined LDB as a result of stars with differing rotation rates depleting lithium slightly earlier or later than our reference case. Our limiting cases for the angular momentum evolution allows us to quantify this rotational “smearing” of the LDB location. The rotational LDB “smearing” is quantified by calculating the difference in bolometric magnitude of the lithium depletion at fixed age. By comparing our no angular momentum loss calculation to the efficient angular momentum loss calculation, we find the difference in bolometric magnitude at fixed age between these calculations is 0.12 and 0.04 mag for young and old clusters, respectively.

In conclusion, since these calculations that include rotation are limiting cases these deviations are conservatively considered as $2\text{-}\sigma$ effects. Thus, rotation negligibly affects the LDB calculation and extent of the observed LDB in comparison to the other sources of theoretical and observational errors. Thus, we do not include a contribution of these effects in the overall error budget for the LDB age technique.

4. Internal Error Budget

Input physics that affect the superadiabatic and radiative regions of the atmosphere dominate the uncertainty in the LDB ages. Qualitatively, results from the previous section imply that the uncertainty in the lithium age dating technique is larger for the higher masses, even though the input physics for the higher masses are relatively more secure. This behavior in the LDB uncertainty is explained in the following way. For a given set of physical inputs, the LDB age as a function of luminosity is a sequence of mass. However, for the lowest masses, variations in the effective temperature of a star move the resulting LDB age–and luminosity–parallel to the sequence in mass. This effect results in the apparent robustness

of the LDB ages to variations in the effective temperature at the low luminosity, low mass end.

The robustness of the LDB ages is best illustrated for the gray atmosphere case (solid line - Figure 5). Using a gray atmosphere, the $M = 0.065 M_{\odot}$ model has a 7% higher effective temperature than the reference model. The 7% increase in the effective temperature results in a 15% decrease in the time for lithium depletion and a 24% increase in the luminosity at the time of lithium depletion. The changes in the lithium depletion luminosity and age are almost identical to changes resulting from a variation in mass. The gray atmosphere $M = 0.065 M_{\odot}$ star has identical lithium depletion luminosity and age as a $M = 0.068 M_{\odot}$ star using the reference Hauschildt, Allard, & Baron (1999) atmosphere. Thus, at fixed luminosity, there is no age difference between these drastically different atmosphere calculations for the lowest mass stars.

Combining the above results to arrive at a theoretical uncertainty in the lithium age-dating technique is difficult. We have treated all variations in the input physics as independent and have not explored correlations between the various input physics or the possibility of nonlinear behavior. Additionally, variations in mixing length, opacity, and atmosphere can all be viewed as variations in the effective temperature. The effective temperature, second only to mass, determines the rate of collapse. Keeping the above in mind, we first attempt to quantify the errors in the LDB ages using the results from Section 3, where we quantify differences in the LDB ages from our reference model that result from changes to the input physics.

The impact on the LDB ages resulting from changes to the input physics, as shown in Figures 3- 5, provides the basis for characterizing the error in the LDB ages as a function of $\log(L)$. Because of the extreme deviation from a realistic change to the input physics, we reduce the deviation for the case of using a zero-metallicity, low temperature opacity (dotted line - Figure 4) by 80%, since a 20% metallicity error is more likely. Assuming the deviation scales linearly with metallicity is conservative since we find a 0.1 dex metallicity variation results in less than 2% age differences overall (see Section 3.4). Among the variations to the input physics, there is no convincing evidence for a preference between older or younger LDB ages in relation to our reference model. Thus, we adopt a symmetric error. We adopt the absolute value of the deviations shown in Figures 3- 5 as $2\text{-}\sigma$ errors. For individual error sources that do not extend the full luminosity range, $-3.0 \lesssim \log(L/L_{\text{dot}}) \lesssim -1.5$, we linearly extrapolate the errors to a value of zero at both luminosity extrema. By adding these deviations in quadrature, we arrive at the total $1\text{-}\sigma$ error in the LDB ages as a function of $\log(L/L_{\odot})$, shown as the solid line in Figure 8.

5. Independent Lithium Depletion Boundary Comparisons

Another way to estimate the systematics in the LDB ages is to compare our result with other independent calculations from the literature. As a first comparison, we compare the reference calculation to the Bildsten et al. (1997) analytical model for lithium depletion. The analytical treatment by Bildsten et al. (1997) requires several assumptions. They assume that the temperature gradient follows the adiabatic temperature gradient for a fully ionized gas, $\nabla_{ad} = 2/5$. Since the largest uncertainty in low mass stellar models arises from determining the effective temperature, Bildsten et al. (1997) treat the effective temperature as a free parameter that is constant during pre-main-sequence contraction. To integrate the lithium destruction over the stellar interior, Bildsten et al. (1997) expand the stellar structure around the central value, and they ignore the change in degeneracy and electron screening as a function of the interior entropy.

Figure 6 shows the percentage age difference at fixed luminosity between the Bildsten et al. (1997) analytical model (their eq. 11) and our reference calculation for the LDB-age relation. A positive difference is in the sense of the analytical model having older ages at fixed luminosity than the reference calculation. To calculate the analytical-model LDB-age relation, we use the same effective temperature and effective molecular weight, $\mu_{eff} \equiv \rho N_A k_B T / P$, at lithium depletion as obtained from the reference calculation and assume a 99% lithium depletion level. The analytical-model results are limited to $M > 0.08 M_\odot$. At the high luminosity end, the analytical model underestimates the LDB age by $\sim 5\%$. For $M \lesssim 0.1 M_\odot$ ($\log(L/L_\odot) \lesssim -2.2$), the effects of degeneracy become important, and the analytical model begins to overestimate the age. Thus, the analytical model follows the numerical results within a numerical constant when degeneracy is not important, but to extend the LDB age technique beyond 90 Myr requires a fully numerical calculation.

The comparison with the analytical model demonstrates the robust nature of the LDB age technique. For an additional characterization of the error in LDB ages, we only use full numerical calculations from the literature that treat the relevant physics more accurately. Figure 7 shows the difference in the lithium depletion age at fixed luminosity for several other calculations. The dotted line compares our results to the calculations of Burrows et al. (1997), the short-dash line is the comparison to Siess et al. (2000), and the four sets of lines with negative age residuals are comparisons to models in given D’Antona & Mazzitelli (1994). The solid line with open squares delineates the comparison with Baraffe et al. (1998), and the open circles show the comparison with the "1998 UPDATE" models of D’Antona & Mazzitelli (1998). With the exception of the calculations from Baraffe et al. (1998), the variations are similar to the trend seen in the internal error budget; the residuals are small at the faint end and increase toward higher masses.

Of the comparisons from the literature, the input physics of Baraffe et al. (1998) are the most similar to ours. The input physics of Baraffe et al. (1998) differ from our reference calculation by their use of the Saumon, Chabrier, & Van Horn (1995) equation of state only, adoption of a mixing length parameter, $\alpha = 1.0$, and a deeper $\tau=100$ fitting point of the outer boundary condition. We do not find any impact on the LDB ages as a result of using only the Saumon, Chabrier, & Van Horn (1995) equation of state (see Section 3.2). Our adoption of a mixing length parameter, $\alpha = 1.0$, results in older LDB ages (see Section 3). Our adoption of the $\tau = 100$ fitting point results in older LDB ages for the youngest clusters, and slightly younger LDB ages for older clusters (see Section 3.4). The calculations of Baraffe et al. (1998) deviate from our reference calculation in a manner that qualitatively resembles our calculation adopting the $\tau = 100$ fitting point. However, the LDB ages of Baraffe et al. (1998) at $\log(L/L_{\odot})=-2.9$ are $5\text{-}\sigma$ younger than our expectations based on the internal error-budget calculation (Figure 8).

The input physics of the D’Antona & Mazzitelli (1994) models differ from our reference model in their use of the MHD equation of state (Däppen et al. 1988) for densities, $\rho < 0.01 \text{ g cm}^{-3}$ and the Magni & Mazzitelli (1979) equation of state otherwise, and a gray atmosphere. The four sets of models compared in Figure 7 are combinations of using either the Alexander & Ferguson (1994) or Kurucz (1998) low temperature opacities and either the mixing length convection theory or the Canuto & Mazzitelli (1991) convection theory. Overall, the four models result in younger LDB ages. The long-dash-dot line shows the comparison that is closest to our reference calculation input physics (Alexander & Ferguson (1994) opacity and mixing length convection theory). Comparing this model to our gray atmosphere calculation (solid line - Figure 5) reveals a remaining difference of 10%. Ignoring implementation differences, we infer the impact of using the Magni & Mazzitelli (1979) equation of state is at most 10%. The long-dash-small-dash line shows the comparison where the only change with the previous model is the Kurucz (1998) low temperature opacity. The largest age difference occurs at $\log(L/L_{\odot})=-2.1$, and this mimics our result when using the Kurucz (1998) opacity (dashed line - Figure 4). The long-dash line is the comparison for the D’Antona & Mazzitelli (1994) model that uses the Alexander & Ferguson (1994) opacity and Canuto & Mazzitelli (1991) convection theory. The short-dash-dot line shows the difference when using the Kurucz (1998) opacity and Canuto & Mazzitelli (1991) convection theory. The published data for the previous set of input parameters end at $M = 0.1M_{\odot}$. The only change to the input physics relevant to the LDB age technique between D’Antona & Mazzitelli (1997) and D’Antona & Mazzitelli (1994) is the convection treatment (Ventura et al. 1998). As we see in the comparison to D’Antona & Mazzitelli (1997) (open circles), the alternative convection treatment has little impact on the LDB ages.

The dotted line compares our reference calculation to that of Burrows et al. (1997).

They employ their own opacity and atmosphere calculations but still have very similar results to our reference calculation. The short-dash line compares our reference calculation to that of Siess et al. (2000). For the atmosphere, they use an analytical fit to the $T(\tau)$ relation calculated by Plez (1992). Their equation of state is based on the framework as outlined in Pols et al. (1995).

6. External Error Budget

An alternative method to calculate the LDB age uncertainty is to use external comparisons with independent lithium depletion calculations from the literature (see Figure 7 and Section 5). We adopt the absolute value of the deviations shown in Figure 7 as $1-\sigma$ errors. We average the individual deviations to arrive at the total $1-\sigma$ error shown as the dashed line in Figure 8. The four calculations from D’Antona & Mazzitelli (1994) are not included in the average since they have been superseded by the more recent D’Antona & Mazzitelli (1997) calculations. For comparisons that do not extend over the entire range of luminosity, we extrapolate by adopting a constant value equal to the comparison endpoints.

The external $1-\sigma$ error is larger than the internal $1-\sigma$ error (Figure 8). The larger external error suggests there are additional systematic deviations in the LDB calculations that result from either numerical differences between the LDB calculations or our calculations have not fully explored the range of relevant physics. However, reconciling the two error estimates only requires an additional 5% error added in quadrature to the internal error estimate. Since we are interested in the impact of input physics uncertainties on the LDB ages only, for the $1-\sigma$ theoretical error in the LDB ages, we adopt the internal $1-\sigma$ errors. Adopting the larger external error may include numerical effects into our error budget. For a simple analytical model of the $1-\sigma$ theoretical error, we adopt a linear trend in $\log(L)$ starting at a value of 8% for $\log(L/L_{\odot})=-1.5$ and decreasing to 3% for $\log(L/L_{\odot})=-3.0$. For luminosities beyond the above luminosity range, we adopt a constant percentage error equal to the endpoint values. The column labeled σ_{THY} in Table 1 gives the $1-\sigma$ error in the reference LDB age as a function of luminosity based on our simple analytical error model.

Taking into account theoretical errors alone, absolute ages of open clusters accurate to 3% for the oldest clusters increasing to 8% for the youngest clusters using the LDB technique are possible. Our calculations of the errors in the LDB age technique show this to be the most accurate method for determining the ages of open clusters. These small errors emphasize the simplicity for calculating the evolutionary rate of fully convective objects powered only by gravitational energy. Even LDB calculations that ignore essential physics (analytical model of Bildsten et al. (1997), ideal gas equation of state, and zero metallicity opacities) have $1-\sigma$

deviations from our reference calculation that are of order 12%. Thus, unless we are ignoring input physics that impact stellar structure of order the error associated with treating the gas physics as an ideal gas, our errors are accurate and are not underestimates.

7. Bolometric Correction

Transformation from a theoretical luminosity or effective temperature to an observable magnitude system requires accurate knowledge of the bolometric correction. A quantitative discussion on the impact of the bolometric correction uncertainty on the derived LDB ages does not exist in the literature. Thus, in this section we briefly characterize this additional error source. There are three methods for bolometric correction determination: empirical, theoretical, and mixed (theoretical method with empirical constraints). Observations for stars of known distance and wide spectral coverage allow an empirical relation between the bolometric magnitude of a star and its broad-band colors (Bessell 1991; Monet et al. 1992). With improved atmospheres, fully theoretical calculations for the bolometric corrections are possible (Hauschildt, Allard, & Baron 1999). A mixture of the theoretical and empirical methods attempts to improve the coverage of bolometric corrections where observations are sparse, by collecting theoretical bolometric calculations and then correcting them empirically (Lejeune, Cuisinier, & Buser 1997).

For our reference bolometric corrections, we choose the theoretical bolometric corrections of Hauschildt, Allard, & Baron (1999). At fixed effective temperature, the top panel in Figure 9 shows the comparison between our reference bolometric corrections and four other bolometric correction determinations. The solid line represents the comparison with the mixed theory/empirical calculations of Lejeune, Cuisinier, & Buser (1997). The difference is in the sense of Lejeune, Cuisinier, & Buser (1997) minus the bolometric corrections of Hauschildt, Allard, & Baron (1999). The long-dash line shows the comparison with the theoretical models used by Lejeune, Cuisinier, & Buser (1997) before applying the empirical corrections. The dash-dot line and short-dash lines compare the results to empirical relations of Monet et al. (1992) and Bessell (1991), respectively. The empirical corrections, in practice, are given as a function of observed photometric color, and blackbody spectral energy distributions fit to the stellar spectra provide the effective temperature scale. Due to the departure from a blackbody, the blackbody fitting method for determining the effective temperature becomes increasingly inaccurate and highly questionable for temperatures < 3000 K (Monet et al. 1992).

The effect on LDB ages for the choice of bolometric correction is shown in the bottom panel of Figure 9. The bolometric correction differences as a function of effective temperature

are mapped to LDB luminosity using the effective temperatures at lithium depletion given in Table 1. For the $1\text{-}\sigma$ error in LDB ages due to bolometric corrections, we take the average absolute value of the percentage age differences shown in the bottom panel of Figure 9 as $1\text{-}\sigma$ deviations. Unlike for the input physics variations, it is not clear which bolometric correction is the best choice. Thus, the bolometric correction error budget is more conservative than the theoretical error budget.

Additionally, there are two sources of systematic error in the bolometric correction when applied to the LDB age technique. Lithium depletion occurs during the pre-main-sequence contraction phase. Thus, the stars at the LDB have smaller $\log(g)$ values than main sequence stars. Since empirical bolometric corrections are derived from main sequence stars, the bolometric corrections are systematically different. Theoretical models used by Lejeune, Cuisinier, & Buser (1997) show the bolometric corrections roughly vary by 0.05 magnitudes per 0.5 dex change in $\log(g)$. The reference calculations have ~ 0.4 dex larger $\log(g)$ values after 1 Gyr. Using bolometric corrections of $\log(g)=5.0$ for stars that actually have $\log(g)=4.5$ results in a 2% overestimate of the LDB ages across all luminosities.

The second source of systematic error in the bolometric correction results from the potential for the stellar cluster to differ in metallicity from the empirical stellar templates employed in determining the bolometric correction. Bolometric corrections vary as a function of metallicity especially for temperatures < 3000 K. The theoretical models used by Lejeune, Cuisinier, & Buser (1997) predict a 0.1 dex change in $[\text{Fe}/\text{H}]$ results in a 4% difference in the resulting LDB ages for the lowest luminosities. The effect is less than 2% toward higher luminosities. These two sources of systematic uncertainty are added in quadrature with the dominant error source based on intercomparisons between alternative bolometric correction determinations as discussed in the preceding paragraph. The resulting $1\text{-}\sigma$ error is shown as the long-dash line in Figure 8.

A comparison of theoretical isochrone fits to the observed color-magnitude diagram of the Pleiades is an additional check to the systematic errors that may be present in the I-band bolometric corrections. For the coolest observed Pleiades members, $T_{\text{eff}}\sim 3400$ K, the isochrone fit is too blue by 0.30 magnitudes in (V-I) when using the Hauschildt, Allard, & Baron (1999) bolometric corrections. The details of this isochrone fit to the Pleiades using the YREC stellar evolution code is given in Pinsonneault et al. (1998). Similar sized discrepancies are generic to all isochrone fits to open cluster color-magnitude diagrams (Grocholski & Sarajedini 2003). If the I-band bolometric correction is solely responsible for the discrepancy in the color-magnitude diagram, revisions to the bolometric corrections of a similar order could be expected. The correction is in the sense of reducing the LDB ages by 19-13%, with the larger impact occurring at the low luminosity/old age end. Alternatively,

the (V-I) colors of the isochrones can be reconciled with the observations by a reduction of $T_{\text{eff}} \sim 150$ K in the isochrones themselves. Reducing the effective temperatures of the reference calculation by 150 K results in a 12% age reduction for the oldest clusters decreasing to a 4% age reduction for the youngest clusters. The reduction in LDB ages is for the bolometric correction only and is independent of the effect the cooler temperatures would have on the theoretical LDB ages.

For a simple analytical $1\text{-}\sigma$ error in the LDB ages resulting from uncertainties in the bolometric correction, we adopt a constant error of 6.0% for $\log(L/L_{\odot}) > -2.6$ and increasing linearly to 10% at $\log(L/L_{\odot}) = -3.0$. The column labeled σ_{BC} in Table 1 gives the $1\text{-}\sigma$ error in the reference LDB ages as a function of luminosity. The last column in Table 1 gives the absolute I-band magnitude of the LDB using the bolometric corrections of Hauschildt, Allard, & Baron (1999). We adopt $M_{\text{bol}\odot} = 4.74$ and reduce the bolometric correction by 0.04 magnitudes to account for the systematically lower gravity at lithium depletion.

8. Conclusion

In conclusion, we employ our error models for the theoretical and bolometric correction uncertainties to rederive LDB ages and errors for the four clusters with previous LDB age determinations (Pleiades - Stauffer, Schultz, & Kirkpatrick (1998); α Per - Stauffer et al. (1999); IC 2391 - Barrado y Navascués, Stauffer, & Patten (1999); NGC 2597 - Oliveira et al. (2003)). We adopt the same apparent I magnitude of the LDB, distance modulus, and reddening as in the original study. Table 2 repeats the observational parameters, along with their adopted errors. We combine the observational errors of the LDB location, reddening, and absolute distance modulus in quadrature to derive the error in the absolute I magnitude of the LDB. The observational error along with the observed LDB luminosity for each cluster is shown as the labeled crosses in Figure 8.

We then calculate the LDB age and errors that result from observational, theoretical, and bolometric correction uncertainties using our reference calculation and error models. The total percentage age error is a sum in quadrature of these three error sources. We derive a LDB age of 148 ± 19 Myr for the Pleiades open cluster. Thus, the LDB age technique rules out ages younger than 91 Myr. For the Pleiades, the difference in the LDB age and the upper main-sequence-fitting age without convective-core overshoot (70-80 Myr - Mermilliod (1981)) is highly significant. Even a maximally plausible 0.30 magnitude change in the I-band bolometric correction (consistent with reconciling the theoretical isochrone fits to the observed (V-I) color of the Pleiades) would result in an age of 126 ± 11 Myr for the Pleiades, where the error includes the observational and theoretical uncertainty only (see Table 2).

Alternative ages and errors of the other open clusters adopting the 0.3 magnitude change in the I-band bolometric correction are given in parenthesis in Table 2.

Our LDB age for the Pleiades is even older than the original LDB age estimate of 125 Myr given in Stauffer, Schultz, & Kirkpatrick (1998). In deriving the Pleiades age, Stauffer, Schultz, & Kirkpatrick (1998) employ the calculations of Baraffe et al. (1998). As discussed in Sections 4 and 6, the lithium depletion calculations of Baraffe et al. (1998) at the lowest luminosities/oldest ages are younger by 15%. The 15% younger age is a $5\text{-}\sigma$ deviation from our reference model based on our examination of the theoretical errors in the LDB ages. Using identical input physics as close as possible to Baraffe et al. (1998), we are unable to reproduce their young LDB ages at the lowest luminosities. Until other independent calculations are available, including an additional 5% error to the LDB ages may be warranted. This systematic error is discussed in Section 6 and is not included in our error budget as it does not materially affect any conclusions.

For the Pleiades cluster, the LDB age technique is dominated by uncertainties in the bolometric correction and the observational LDB location. If the bolometric correction and LDB location error sources are eliminated, then our calculations show the LDB age technique could provide absolute ages for open clusters accurate to 3% for 200 Myr clusters increasing to 8% for 20 Myr clusters.

We want to thank I. Baraffe, J. Stauffer, and D. Terndrup for useful discussions. This work was supported by NSF grant AST-0206008.

REFERENCES

- Allard, F., Hauschildt, P. H., Alexander, D. R., Tamanai, A., & Schweitzer, A. 2001, *ApJ*, 556, 357
- Alexander, D. R. & Ferguson, J. W. 1994, *ApJ*, 437, 879
- Alexander, D. R., Johnson, H. R., & Rypma, R. L. 1983, *ApJ*, 272, 773
- Andersen, J., Nordström, B., & Clausen, J. V. 1990, *ApJ*, 363, L33
- Baraffe, I., Chabrier, G., Allard, F., & Hauschildt, P. H. 1998, *A&A*, 337, 403
- Barrado y Navascués, D., Stauffer, J. R., & Patten, B. M. 1999, *ApJ*, 522, L53
- Bessell, M. S. 1991, *AJ*, 101, 662

- Bildsten, L., Brown, E. F., Matzner, C. D., & Ushomirsky, G. 1997, *ApJ*, 482, 442
- Burke, C. J., & Pinsonneault, M. H. 2000, in *Bull. AAS* 32, ed. R. W. Milkey (Melville: AIP), 1462
- Burrows, A., et al. 1997, *ApJ*, 491, 856
- Canuto, V. M., & Mazzitelli, I. 1991, *ApJ*, 370, 295
- Chabrier, G., Baraffe, I., & Plez, B. 1996, *ApJ*, 459, L91
- Chabrier, G., Baraffe, I., Allard, F., & Hauschildt, P. 2000, *ApJ*, 542, 464
- Däppen, W., Mihalas, D., Hummer, D. G., & Mihalas, B. W. 1988, *ApJ*, 332, 261
- D’Antona, F., & Mazzitelli, I. 1994, *ApJS*, 90, 467
- D’Antona, F., & Mazzitelli, I. 1997, *Mem.S.A.It.*, 68, 807
- D’Antona, F., & Mazzitelli, I. 1998, in *ASP Conf. Ser.* 134, *Brown Dwarfs and Extrasolar Planets*, eds. R. Rebolo, E. L. Martín, M. R. Zapatero Osorio (San Francisco: ASP), 442
- Demarque, P., Sarajedini, A., & Guo, X. -J. 1994, *ApJ*, 426, 165
- Grevesse, N., & Noels, A. 1993, in *Origin and Evolution of the Elements*, ed. N. Prantzos, E. Vangioni-Flam, & M. Cassé (Cambridge: Cambridge Univ. Press), 15
- Grocholski, A. J., & Sarajedini, A. 2003, *MNRAS*, in press
- Guenther, D. B., Demarque, P., Kim, Y.-C., & Pinsonneault, M. H. 1992, *ApJ*, 387, 372
- Guillot, T., Chabrier, G., Gautier, D., & Morel, P. 1995, *ApJ*, 450, 463
- Hauschildt, P. H., Allard, F., & Baron E. 1999, *ApJ*, 512, 377
- Iglesias, C. A. & Rogers, F. J. 1996, *ApJ*, 464, 943
- Jeffries, R. D. & Naylor T. 2001, in *ASP Conf. Ser.* 243, *From Darkness to Light: Origin and Evolution of Young Stellar Clusters*, eds. T. Montmerle, & P. André (San Francisco: ASP), 633
- Kippenhahn R. & Weigert A. 1990, *Stellar Structure and Evolution*, (Berlin: Springer-Verlag)

- Kurucz, R. L. 1998, in IAU Symp. 189, Fundamental Stellar Properties: The Interaction between Observation and Theory, eds. T. R. Bedding, A. J. Booth, & J. Davis, (Dordrecht: Kluwer), 217
- Lejeune, T., Cuisinier, F., & Buser, R. 1997, A&AS, 125, 229
- Ludwig, H. -G., Freytag, B., & Steffen, M. 1999, A&A, 346, 111
- Magni, G., & Mazzitelli, I. 1979, A&A, 72 134
- Mermilliod, J. -C. 1981, A&A, 97, 235
- Monet, D. G., Dahn, C. C., Vrba, F. J., Harris, H. C., Pier, J. R., Luginbuhl, C. B., & Ables, H. D. 1992, AJ, 103, 638
- Oliveira, J. M., Jeffries, R. D., Devey, C. R., Barrado y Navascués, D., Naylor, T., Stauffer, J. R., Totten, E. J. 2003, MNRAS, 342, 651
- Pinsonneault, M. H., Stauffer, J., Soderblom, D. R., King, J. R., & Hanson, R. B. 1998, ApJ, 504, 170
- Plez, B. 1992, A&AS, 94, 527
- Pols, O. R., Tout, C. A., Eggleton, P. P., & Han, Z. 1995, MNRAS, 274, 964
- Potekhin, A. Y., Baiko, D. A., Haensel, P., & Yakovlev, D. G. 1999, A&A, 346, 345
- Potekhin, A. Y., Chabrier, G., & Yakovlev, D. G. 1997, A&A, 323, 415
- Rogers, F. J., & Nayfonov, A. 2002, ApJ, 576, 1064
- Rogers, F. J., Swenson, F. J., & Iglesias, C. A. 1996, ApJ, 456, 902
- Saumon, D., Chabrier, G., & Van Horn, H. M. 1995, ApJS, 99, 713
- Siess, L., Dufour, E., & Forestini, M. 2000, A&A, 358, 593
- Sills, A., Pinsonneault, M. H., Terndrup, D. M. 2000, ApJ, 534, 335
- Stahler, S. W. 1988, ApJ, 332, 804
- Stahler, S. W., Palla, F., & Salpeter, E. E. 1986, ApJ, 302, 590
- Stassun, K. G., & Terndrup, D. M. 2003, PASP, 115, 505

- Stauffer, J. R., Jeffries, R. D., Martín, E. L., & Terndrup, D. M. 2000, in ASP Conf. Ser. 223, 11th Cambridge Workshop on Cool Stars, Stellar Systems and the Sun, eds. R. J. Garcia Lopez, R. Rebolo, and M. R. Zapaterio Osorio (San Francisco: ASP), 399
- Stauffer, J. R., Schultz, G., & Kirkpatrick, J. D. 1998, ApJ, 449, L199
- Stauffer, J. R., et al. 1999, ApJ, 527, 219
- Terndrup, D. M., Stauffer, J. R., Pinsonneault, M. H., Sills, A., Yuan, Y., Jones, B. F., Fischer, D., & Krishnamurthi, A. 2000, AJ, 119, 1303
- Ventura, P., Zeppieri, A., Mazzitelli, I., & D’Antona, F. 1998, A&A, 334, 953
- Vitense, E. 1953, Z. Astrophys., 32, 135

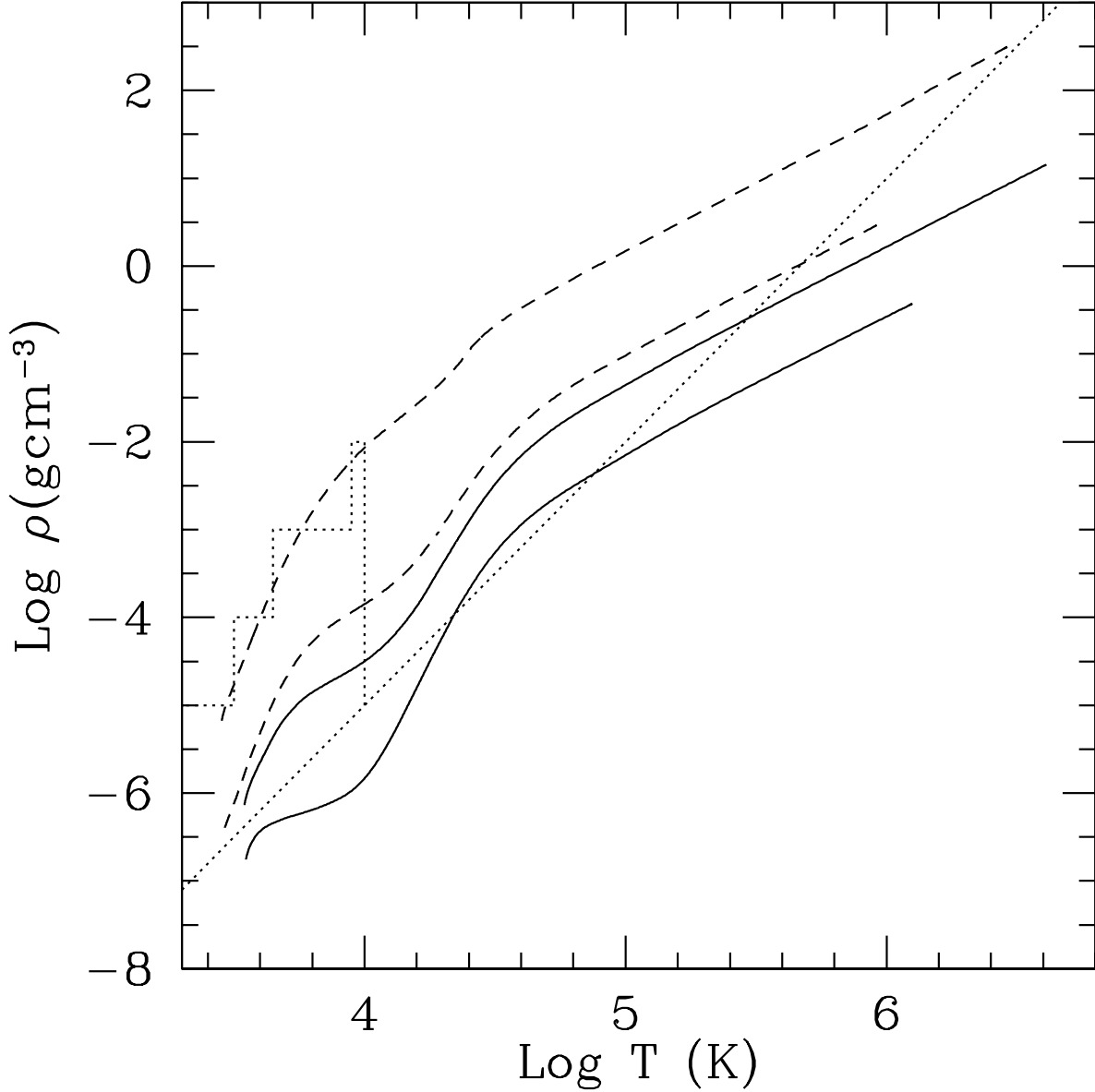


Fig. 1.— Solid lines are the run of density as a function of temperature for $M=0.30 M_{\odot}$ for the initial and lithium depletion models, bottom and top respectively. Dashed lines show the run of density for the $M=0.065 M_{\odot}$ models. The diagonal dotted line represents the upper density boundary at $R \equiv \rho/T_6^3 = 1$ for the Alexander & Ferguson (1994) low temperature and Iglesias & Rogers (1996) high temperature opacities used in the reference calculations. The dotted line extending to higher densities shows the Alexander, Johnson, & Rypma (1983) molecular opacity table boundaries.

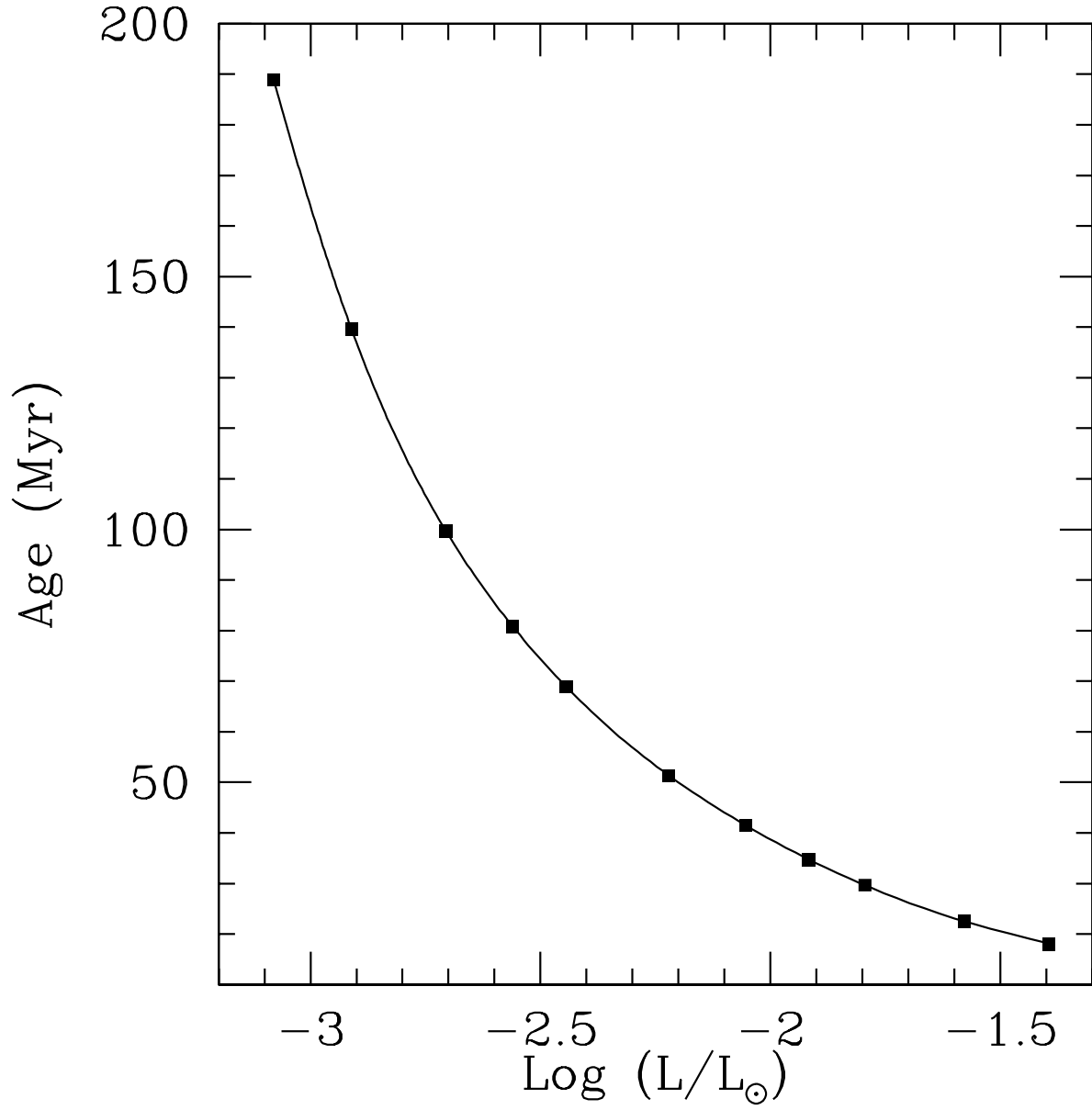


Fig. 2.— Reference lithium depletion age as a function of luminosity.

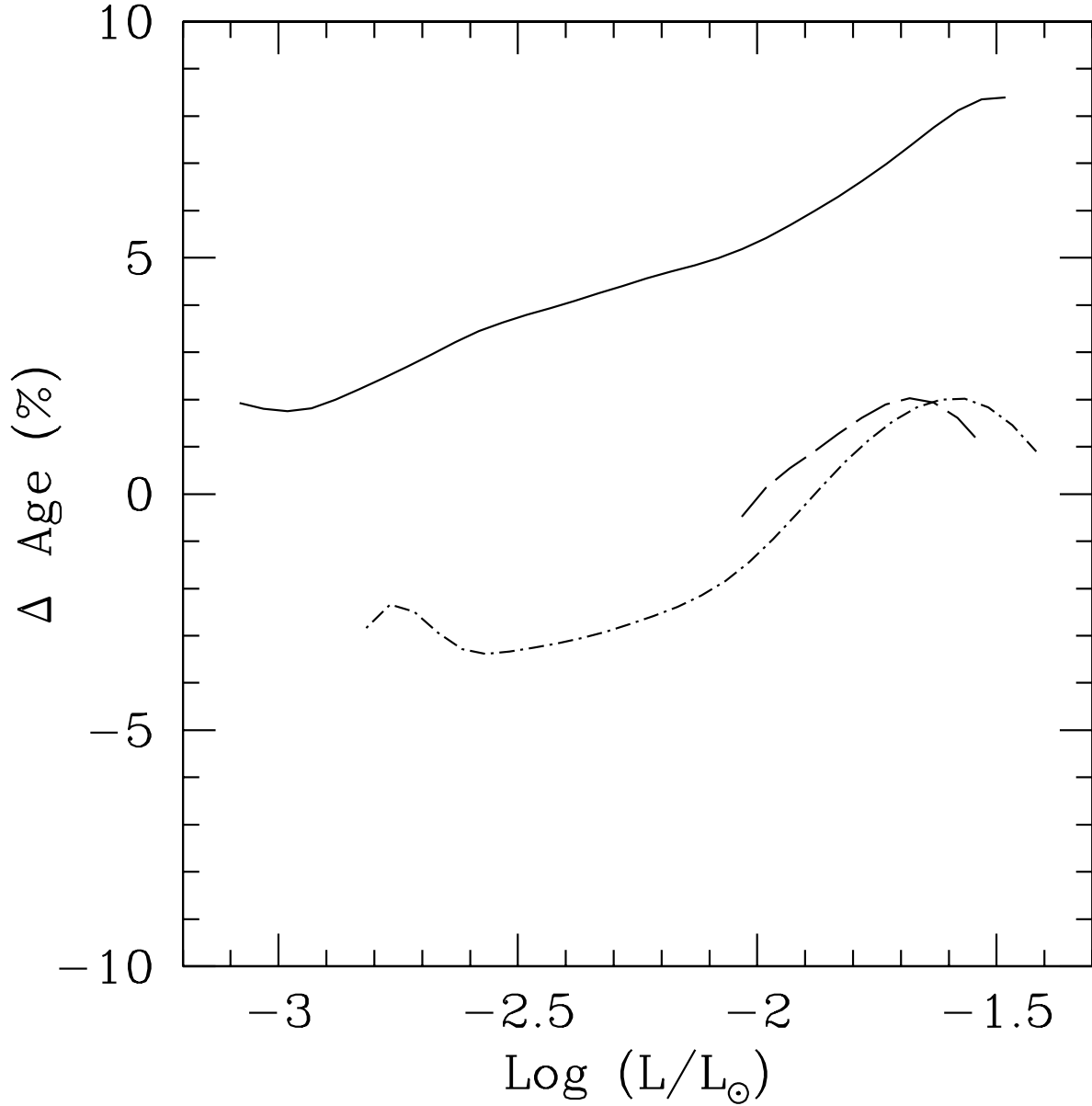


Fig. 3.— Solid line shows the percentage difference in the LDB ages between adopting the mixing length parameter, $\alpha = 1.0$ and the solar calibrated, $\alpha = 1.75$, reference model. A positive difference is in the sense that the parameter variation gives an older LDB age than the reference model. Dashed line shows the percentage difference in the LDB ages obtained by adopting the MHD equation of state. The upper density limit of the MHD equation of state restricts calculations to $M/M_{\odot} > 0.175$. The line has been shifted $\Delta \text{Log}(L) = -0.1$ for better visibility. Dashed-dot line shows the percentage difference in the LDB ages obtained by adopting the OPAL 2001 equation of state (Rogers & Nayfonov 2002). The limits of the table restricts calculations to $M/M_{\odot} > 0.08$.

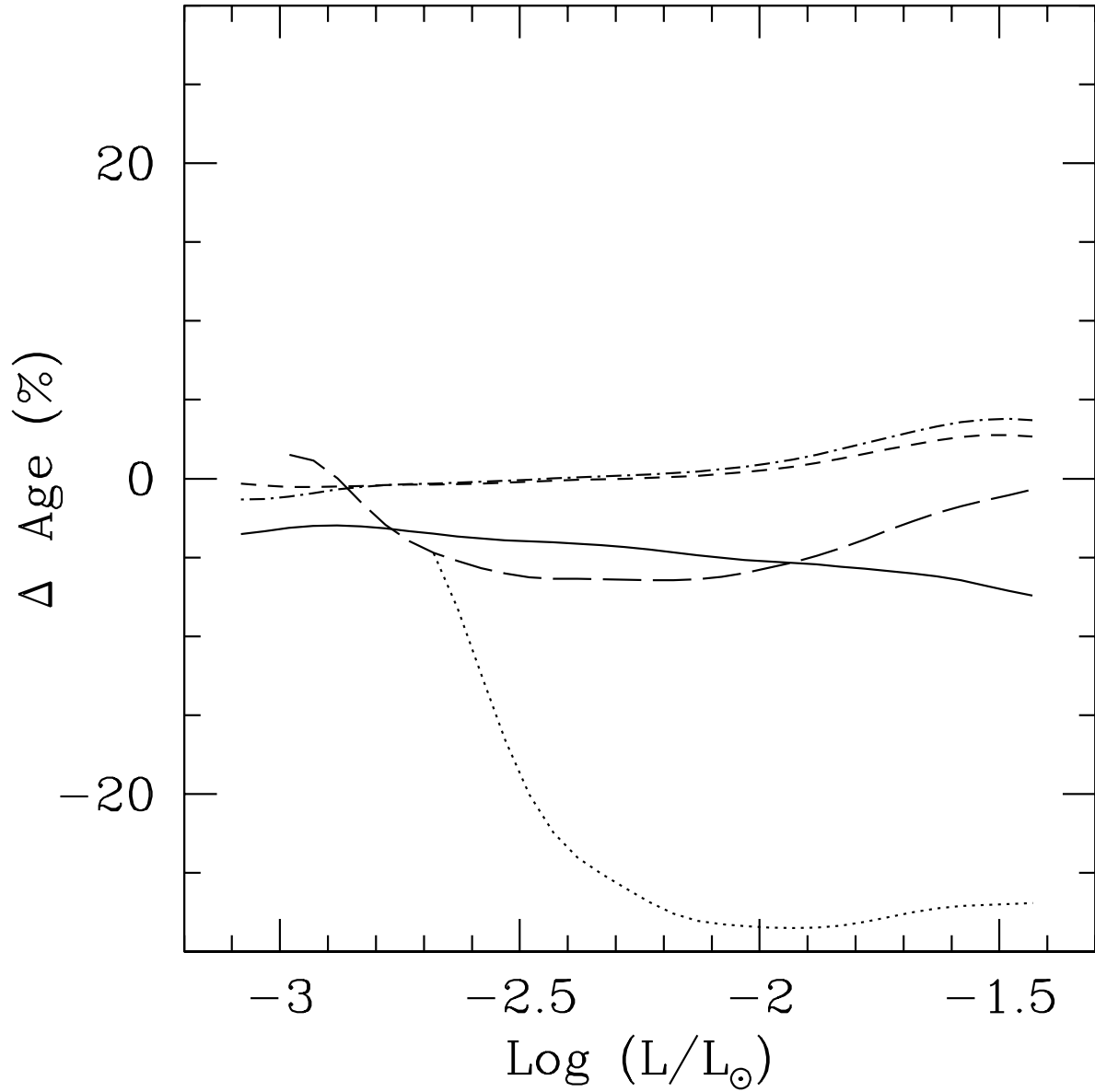


Fig. 4.— Solid line shows the percentage difference in the LDB ages obtained by enforcing the adiabatic temperature gradient. The dashed line shows the difference using the Kurucz (1998) low temperature opacity. The short-dashed line shows the LDB age difference using the Allard et al. (2001) dusty opacities. The dot-dashed line compares the LDB age using the high opacity. The dotted line is for a zero metallicity opacity.

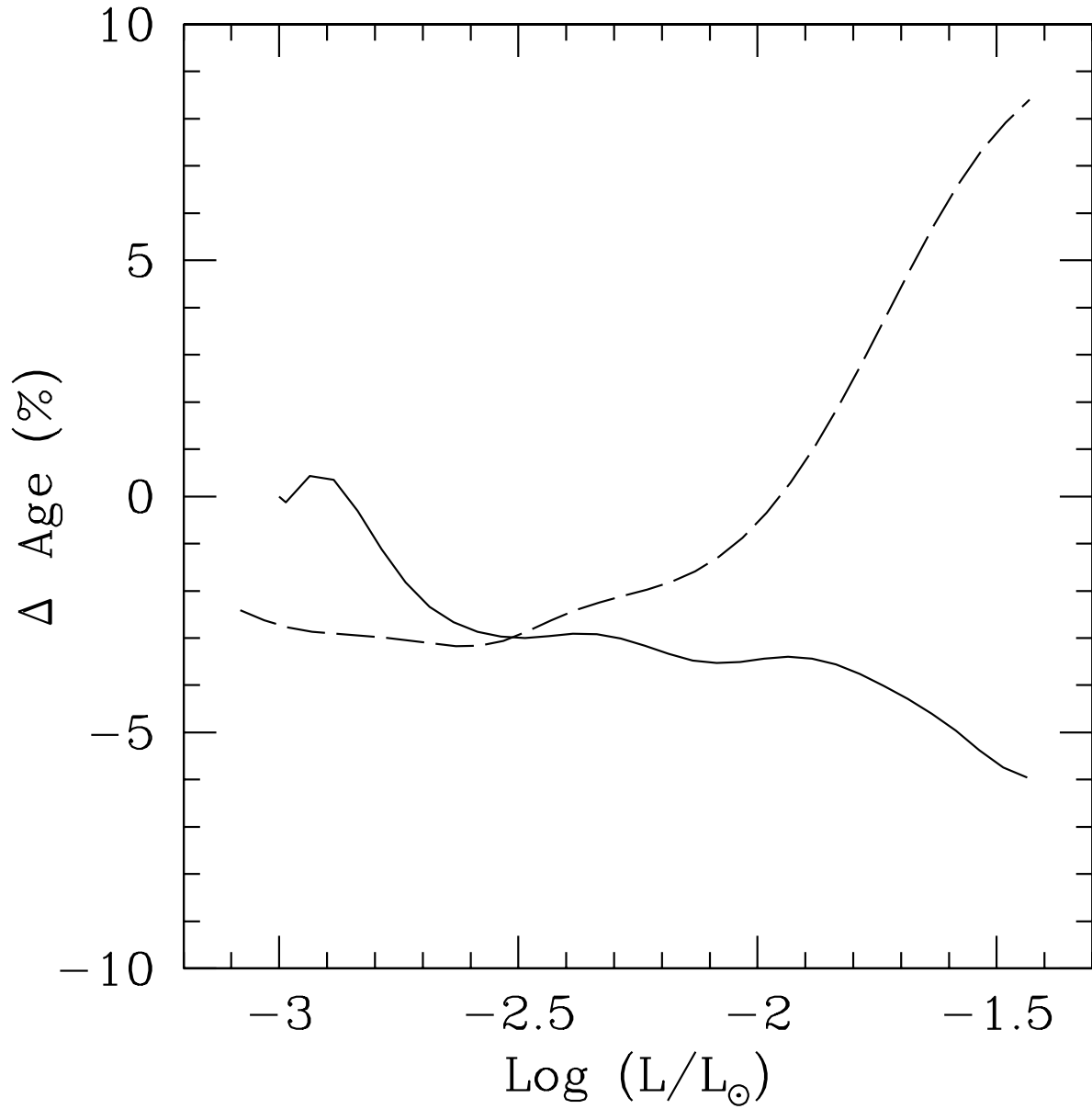


Fig. 5.— Solid line shows the percentage difference in the LDB ages obtained by using the gray atmosphere. Shows the LDB age adopting a $\tau = 100$ fitting point for the boundary condition.

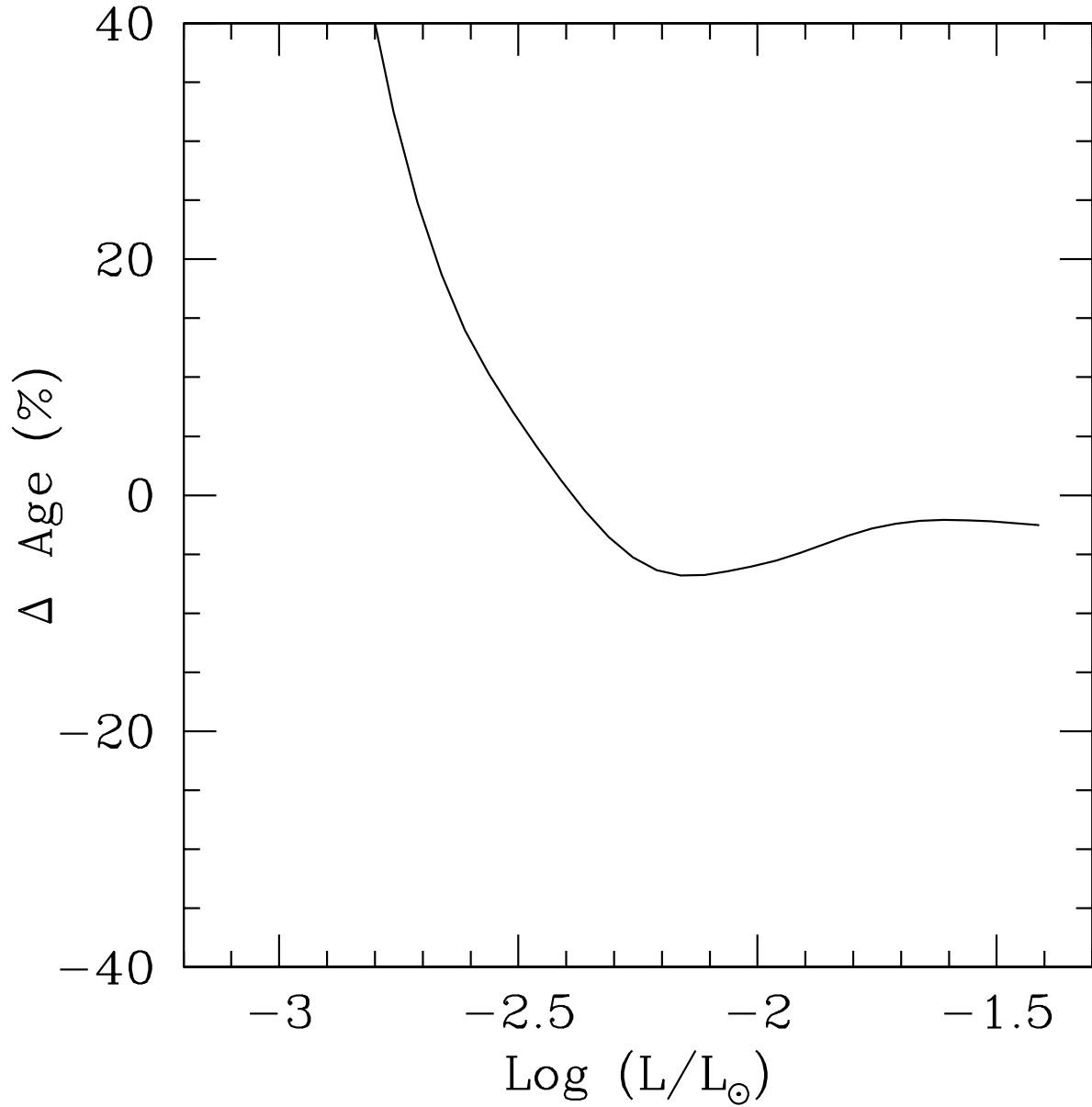


Fig. 6.— Percentage difference in the LDB ages between the analytical model of Bildsten et al. (1997) and the numerical reference model. A positive difference is in the sense that the analytical model gives an older LDB age than the reference model.

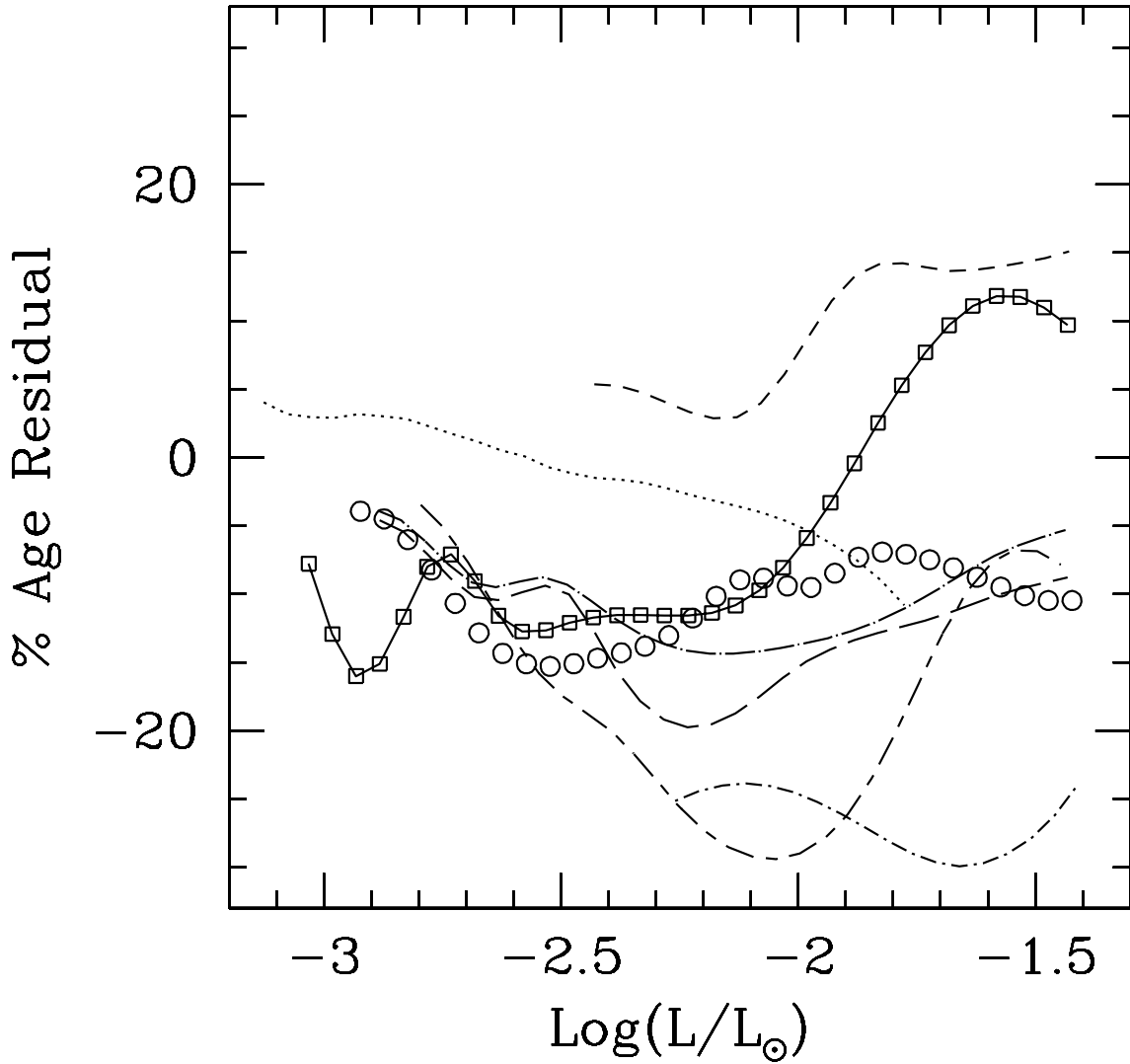


Fig. 7.— Percentage difference in the LDB ages between the reference model and independent LDB age calculations from the literature. Short-dashed line is the comparison with Siess et al. (2000). Dotted line is the comparison with Burrows et al. (1997). The four remaining lines are comparisons to different model assumptions in D’Antona & Mazzitelli (1994). The solid line with open squares delineate the comparison with the calculations of Baraffe et al. (1998), and the open circles shows the comparison to the calculation of D’Antona & Mazzitelli (1998).

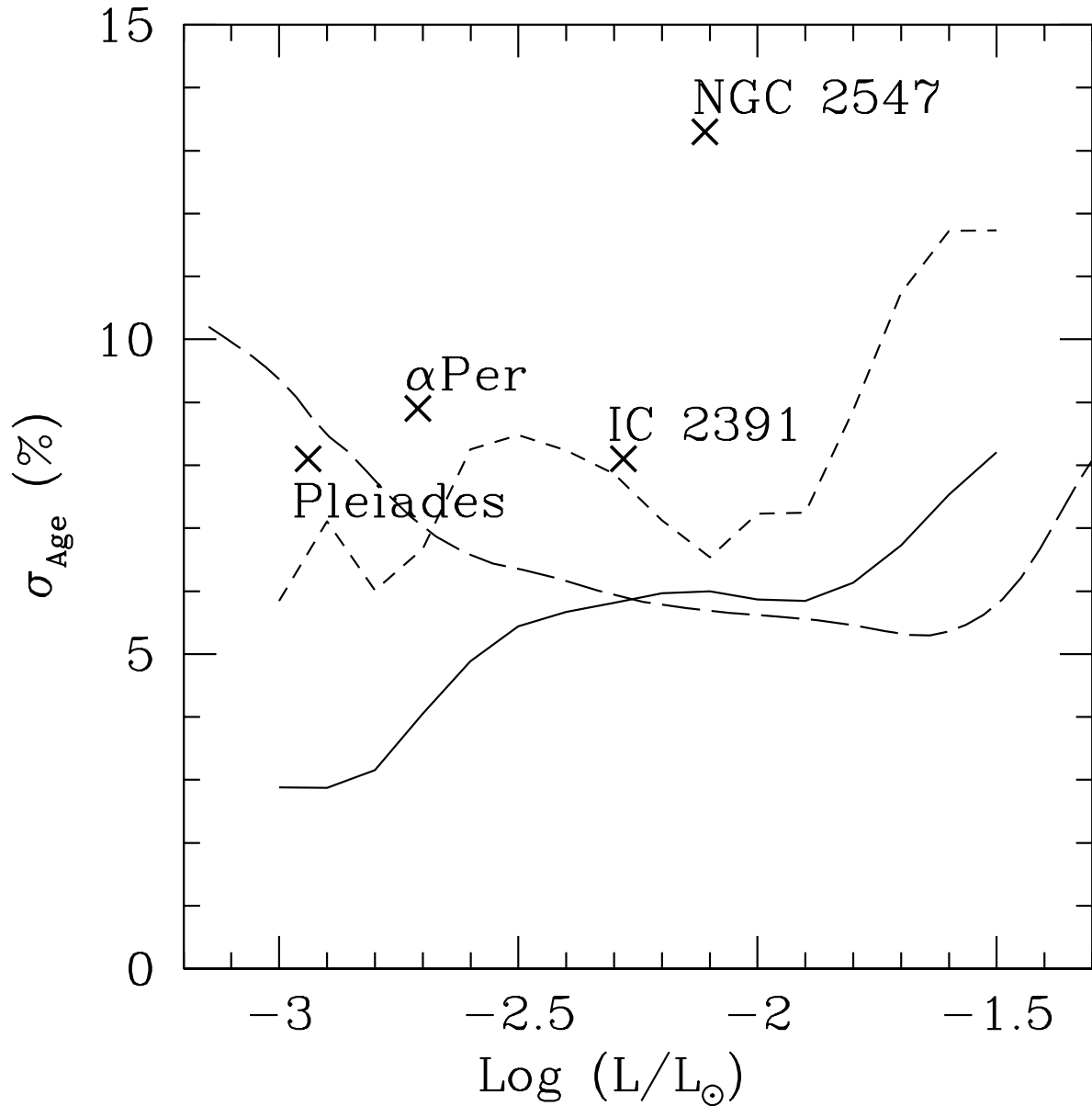


Fig. 8.— Percentage, 1- σ uncertainty in the LDB age as a function of $\log(L/L_{\odot})$. Solid line and short-dash line shows the theoretical uncertainty based on deviations from the reference model for changes to the input physics and for comparisons to independent calculations from the literature, respectively. Long-dash line is the uncertainty that results from bolometric correction uncertainties. Crosses point out the observed luminosity of the LDB and the age uncertainty resulting from the uncertainty in its location for the labeled open clusters.

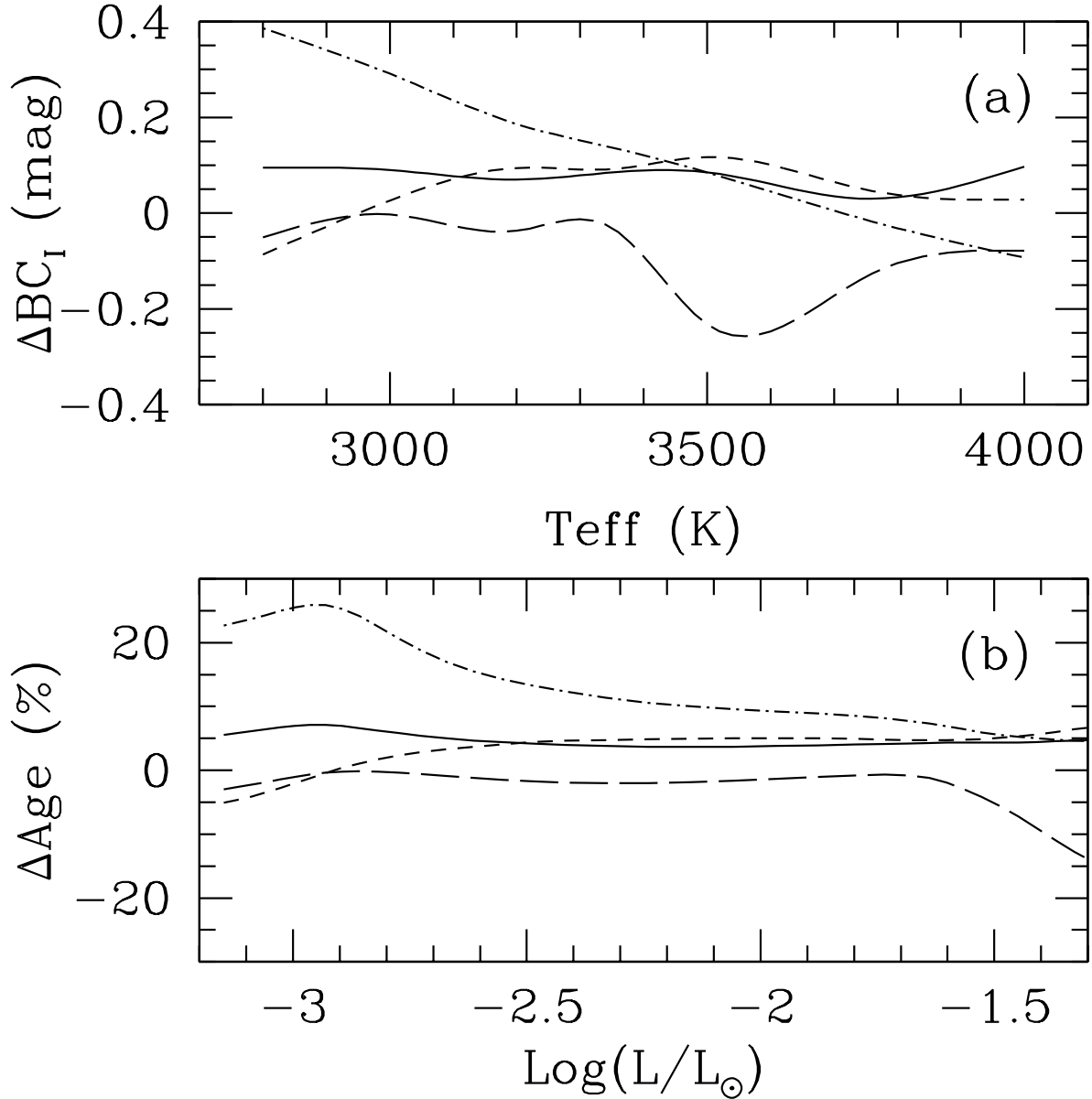


Fig. 9.— **a** Magnitude difference in the I-band bolometric correction at fixed effective temperature between several other determinations and the theoretical calculations of Hauschildt, Allard, & Baron (1999). The solid line compares with the empirically corrected calculations of Lejeune, Cuisinier, & Buser (1997). The difference is in the sense of Lejeune, Cuisinier, & Buser (1997) minus Hauschildt, Allard, & Baron (1999). The long-dash line shows the comparison with the theoretical models used by Lejeune, Cuisinier, & Buser (1997) before applying the empirical corrections. The dash-dot line and short-dash lines compare the results to empirical relations of Monet et al. (1992) and Bessell (1991), respectively. **b** Percentage difference in the LDB ages at fixed $\text{log}(L/L_{\odot})$ in comparison to the adopted Hauschildt, Allard, & Baron (1999) bolometric corrections. Line types are identical to the top panel.

Table 1. Reference Li Depletion Data^a

| M/M_{\odot} | Age (Myr) | $\text{Log}(L/L_{\odot})$ | $\text{Log}(R/R_{\odot})$ | $\text{Log}(g)$ | $\text{Log}(\text{Teff})$ | σ_{THY} (% Age) | σ_{BC} (% Age) | M_I |
|---------------|--------------|---------------------------|---------------------------|-----------------|---------------------------|---------------------------|--------------------------|-------|
| 0.30 | 18.08 | -1.39 | -0.253 | 4.42 | 3.54 | 8.0 | 6.0 | 7.84 |
| 0.25 | 22.53 | -1.58 | -0.321 | 4.48 | 3.53 | 7.7 | 6.0 | 8.37 |
| 0.20 | 29.67 | -1.80 | -0.406 | 4.55 | 3.52 | 7.0 | 6.0 | 8.98 |
| 0.175 | 34.76 | -1.92 | -0.458 | 4.60 | 3.51 | 6.6 | 6.0 | 9.30 |
| 0.15 | 41.53 | -2.05 | -0.519 | 4.65 | 3.51 | 6.2 | 6.0 | 9.64 |
| 0.125 | 51.37 | -2.22 | -0.593 | 4.72 | 3.50 | 5.6 | 6.0 | 10.10 |
| 0.10 | 68.88 | -2.44 | -0.689 | 4.82 | 3.50 | 4.9 | 6.0 | 10.70 |
| 0.09 | 80.89 | -2.56 | -0.738 | 4.87 | 3.49 | 4.5 | 6.0 | 11.04 |
| 0.08 | 99.62 | -2.70 | -0.796 | 4.93 | 3.48 | 4.0 | 7.0 | 11.45 |
| 0.07 | 139.6 | -2.91 | -0.871 | 5.03 | 3.47 | 3.3 | 9.1 | 12.09 |
| 0.065 | 188.8 | -3.08 | -0.924 | 5.10 | 3.45 | 3.0 | 10.8 | 12.64 |

^aLi depleted by a factor of 100 from initial value

Table 2. Observed Cluster Properties

| Cluster | I_{LDB} | σ_{LDB} | $(m - M)_o$ | σ_{DM} | A_I | σ_A | M_I | σ_M | Age ^a (Myr) | σ_{OBS} (% Age) | σ_{THY} (% Age) | σ_{BC} (% Age) | σ_{TOT} (% Age) | σ_{AGE} ^b (Myr) |
|--------------|-----------|----------------|-------------|---------------|-------|------------|-------|------------|---------------------------|---------------------------|---------------------------|--------------------------|---------------------------|--------------------------------------|
| Pleiades | 17.86 | 0.10 | 5.60 | 0.10 | 0.06 | 0.03 | 12.20 | 0.14 | 148 (126) | 8.1 | 3.2 | 9.4 | 13 | 19 (11) |
| α Per | 17.87 | 0.15 | 6.23 | 0.10 | 0.17 | 0.04 | 11.47 | 0.18 | 101 (87) | 8.9 | 4.0 | 7.1 | 12 | 12 (9) |
| IC 2391 | 16.22 | 0.15 | 5.95 | 0.10 | 0.02 | 0.02 | 10.25 | 0.18 | 55 (48) | 8.1 | 5.4 | 6.0 | 11 | 6 (5) |
| NGC 2547 | 18.00 | 0.25 | 8.15 | 0.15 | 0.05 | 0.03 | 9.80 | 0.29 | 45 (38) | 13.3 | 6.0 | 6.0 | 16 | 7 (7) |

^aValue in parenthesis is the LDB age for a -0.3 magnitude shift in the I-band bolometric correction (see Section 7).

^bValue in parenthesis is the error in the LDB age for a -0.3 magnitude shift in the I-band bolometric correction. This error includes observational and theoretical errors only.